

# Prolonged and gradual recovery of metazoan-algal reefs following the end-Permian mass extinction

Brian M. Kelley<sup>1,\*</sup>, Meiyi Yu<sup>2</sup>, Daniel J. Lehrmann<sup>3</sup>, Demir Altiner<sup>4</sup>, and Jonathan L. Payne<sup>5</sup>

<sup>1</sup>Department of Geosciences, Penn State University, University Park, Pennsylvania 16802, USA

<sup>2</sup>Department of Resources and Environmental Engineering, Guizhou University, Caijiaguan, Guiyang 550003, Guizhou Province, P.R. China

<sup>3</sup>Geosciences Department, Trinity University, San Antonio, Texas 78212, USA

<sup>4</sup>Department of Geological Engineering, Middle East Technical University, Ankara, 06800, Turkey

<sup>5</sup>Department of Earth and Planetary Sciences, Stanford University, Stanford, California 94305, USA

## ABSTRACT

The tempo of biotic recovery following extinction reflects the time scales of evolutionary processes and the long-term consequences of degraded ecosystems, but recovery patterns are poorly resolved. In this study, we investigated the tempo of biotic recovery by evaluating metazoan-algal reef assembly following the end-Permian mass extinction. We combined satellite imagery analysis, field mapping, biostratigraphy, and quantitative petrography to assess recovery in the oldest-known and most stratigraphically extensive Lower to Middle Triassic platform-margin reef. The reef occurs in upper Spathian (upper Lower Triassic) to upper Anisian (lower Middle Triassic) strata of the Great Bank of Guizhou (GBG) isolated carbonate platform in south China. Previous work suggests that metazoan-algal reefs were absent for 8–10 m.y. following extinction but were biologically diverse from their Pelsonian (middle Anisian) initiation. This pattern implies that reefs can reassemble rapidly ( $\ll 1$  m.y.) when environmental conditions are favorable. In contrast, our analyses indicate that calcareous sponges, calcareous algae, and early scleractinian corals occurred progressively in the GBG reef and that biotic recovery metrics increased gradually. Unlike nonreef ecosystems, biodiverse metazoan-algal reefs were delayed until the late Pelsonian or early Illyrian, postdating broader marine ecosystem recovery and isotopic evidence for carbon-cycle stabilization by 2–4 m.y. Our findings suggest that reef and nonreef ecosystems differ in their recovery pattern and tempo. Reef recovery from severe environmental perturbation can require several million years, even after hospitable conditions return, highlighting the importance of modern reef conservation.

## INTRODUCTION


The pace of biotic recovery following extinction reflects the tempo of evolutionary processes and the potential long-term consequences of ecosystem degradation, but recovery patterns and rates are poorly constrained. The recovery of reef ecosystems from mass extinction offers the opportunity to assess the tempo of ecosystem assembly following severe environmental perturbation and to evaluate how recovery tempo differs for biodiverse ecosystems with high levels of integration. During the end-Permian mass extinction, Paleozoic reef builders, including rugose and tabulate corals, calcareous sponges,

and calcareous algae, suffered total or near-total extinction (Flügel, 2002). In the aftermath, biodiverse metazoan-algal reefs were absent for 8–10 m.y. (Martindale et al., 2019). The redevelopment of biodiverse reefs is considered a final step in marine ecosystem recovery from extinction (Erwin, 1998), but the pattern and tempo of metazoan-algal reef recovery in the aftermath of the end-Permian extinction remain poorly constrained, leaving the broader Triassic recovery pattern unresolved.

Triassic reef recovery (Fig. 1) is characterized as a stepwise progression from Lower Triassic microbial to Middle Triassic metazoan-algal reefs (Stanley, 1988; Flügel, 2002; Martindale et al., 2019). Lower Triassic buildups characterized as reefs are dominated by microbial mounds and rare meter-scale buildups of sponges or

bivalves, but scleractinian corals are absent (e.g., Pruss et al., 2007; Brayard et al., 2011; Marengo et al., 2012; Heindel et al., 2018; Baud et al., 2021). In contrast, Anisian (lower Middle Triassic) reefs include a greater diversity of framework builders, including calcareous sponges, calcareous algae, and the earliest scleractinian corals (Flügel, 2002). These biodiverse assemblages of metazoans and algae—more broadly recognized as reefs—have not been observed in strata older than the Pelsonian (middle Anisian) (Morycowa and Szulc, 2010). The recurrence of coral-sponge-algal reefs has been regarded as geologically rapid (Flügel and Senowbari-Daryan, 2001; Flügel, 2002), implying that biodiverse benthic ecosystems with high levels of integration can develop over geologically short time scales ( $\ll 1$  m.y.). Alternatively, the apparently rapid reassembly of metazoan-algal reefs could result from limitations of the fossil record because lower Mesozoic reefs are rare and limited in stratigraphic extent (Fig. 1).

In this study, we assessed the timing and tempo of metazoan-algal reef recovery from the end-Permian extinction in the most stratigraphically extensive and oldest Triassic platform-margin reef—the Great Bank of Guizhou (GBG) reef in south China (Figs. 1 and 2). The GBG reef provides an opportunity to constrain Triassic reef recovery because of its exceptional exposure, upper Spathian to upper Anisian stratigraphic range, biostratigraphic constraints from foraminifers, and chemostratigraphic constraints from  $\delta^{13}\text{C}$  analyses (Kelley et al., 2020). In addition, a biostratigraphic and geochronologic framework from the adjacent Guandao basin-margin section (Lehrmann et al., 2015; Altiner et al., 2021) provides a robust reef age model.

Brian Kelley  <https://orcid.org/0000-0003-4203-1481>  
\*brian.kelley@psu.edu

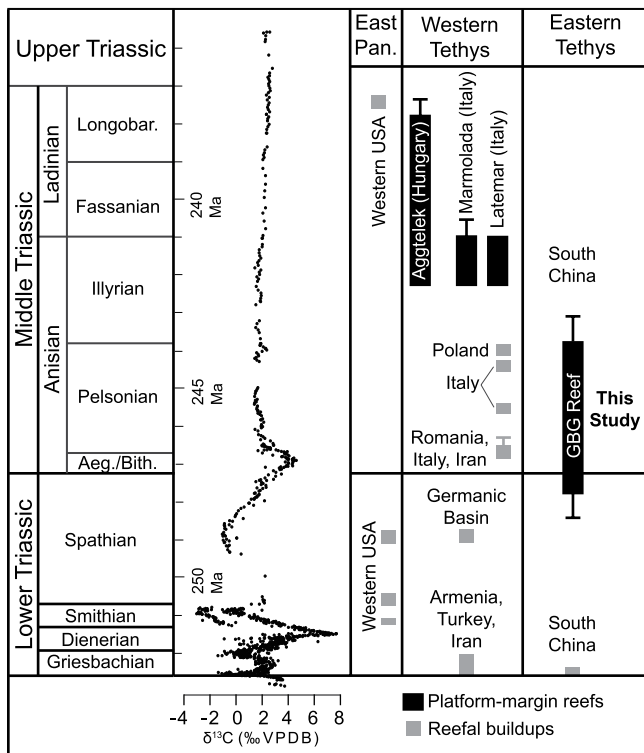


**Figure 1. Early Mesozoic reef stratigraphic ranges, based on Flügel (2002), Martindale et al. (2019), Baud et al. (2021), Wu et al. (2022), Heuer et al. (2022), and references therein, with  $\delta^{13}\text{C}$  values from Payne et al. (2004). Abbreviations: Pan.—Panthalassa; Longobar.—Longobardian; Aeg.—Aegean; Bith.—Bithynian; VPDB—Vienna Peedee belemnite; GBG—Great Bank of Guizhou.**

## METHODS

To assess GBG reef development, we integrated *WorldView-1* satellite imagery analysis, field observations, foraminifer biostratigraphy, and quantitative petrography. Although discontinuous exposure and the rarity of field-observable reef bedding prevented sampling along linear stratigraphic sections, sample locations were constrained by global positioning system (GPS) measurements, satellite imagery, and topographic maps. Samples were placed in stratigraphic order (Fig. 3A) using bedding observed in satellite imagery (Fig. 3B). Although this approach introduced uncertainty in stratigraphic position, an error of 25 m (for example) represents a stratigraphic error of only ~2%. Errors of this size would not substantially alter trends in fossil occurrences or recovery metrics, and the integrated positioning approach makes errors of greater magnitude unlikely.

The reef was subdivided into three zones (Fig. 3) to determine if statistically significant changes in recovery metrics occur across adjacent zones (more rapid recovery) or nonadjacent zones (more gradual recovery). The reef zones included zone 1 (reef base to the first occurrence of metazoan framework), zone 2 (metazoan framework to the base of the Upper Reef), and zone 3 (Upper Reef). These zones represent the most evident transitions in reef composition, making the zonal statistical analyses more conservative.

To document fossil occurrences, abundance, and body size, we combined field observations with petrographic analysis of 164 hand samples and thin sections. Fossil occurrences were tabulated (Fig. 3), and well-preserved reef boundstone was selected for point counting (32 samples; 300 points per sample) using the grain-solid method (Flügel, 2010). We estimated body size by measuring fossils along their maximum linear dimension, a metric that explains ~85% of the variance in fossil volume (Novack-Gottshall, 2008).

## GEOLOGIC SETTING

The GBG is a Changhsingian (uppermost Permian) to lower Carnian (lowermost Upper Triassic) isolated carbonate platform in the Nanpanjiang Basin of south China (Figs. 2A–2C). The platform margin at Bianyang is exceptionally exposed in cross section by exhumation along a syncline (Figs. 2D and 2E). The reef initiated in the upper Spathian (Payne et al., 2006) and persisted in situ to upper Pelsonian or lower Illyrian strata (Kelley et al., 2020), reaching a stratigraphic thickness of ~900 m (Lehrmann et al., 1998). The reef facies is characterized by the occurrence

of *Tubiphytes* boundstone. *Tubiphytes* is an automicritic fossil of uncertain taxonomic position (Senowbari-Daryan, 2013), attributed to microbial micrite precipitation associated with uncalcified algae (Payne et al., 2006). The reef reflects two depositional intervals, as indicated by progradation of the Upper Reef facies (Fig. 2E), with an uncertain potential depositional hiatus between the two intervals. The reef facies is relatively continuous around the GBG margin (Lehrmann et al., 1998) and was deposited along prograding slope clinoforms from the outer margin to the lower slope (Kelley et al., 2020).

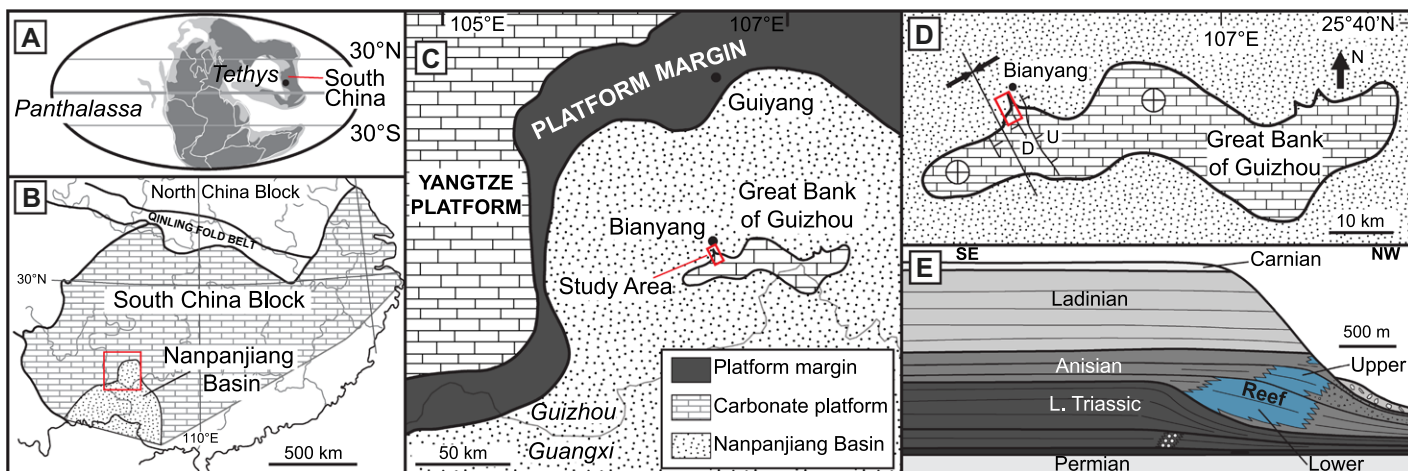


**Figure 2. Geologic setting, modified from Scotese (2014) and Kelley et al. (2020). (A) Early Mesozoic paleogeography. (B) South China block and Nanpanjiang Basin. Red square is extent of C. (C) Nanpanjiang Basin detail and Great Bank of Guizhou (GBG) location. (D) Bianyang and GBG platform-margin location. Red square is extent of E. (E) Platform and reef architecture.**



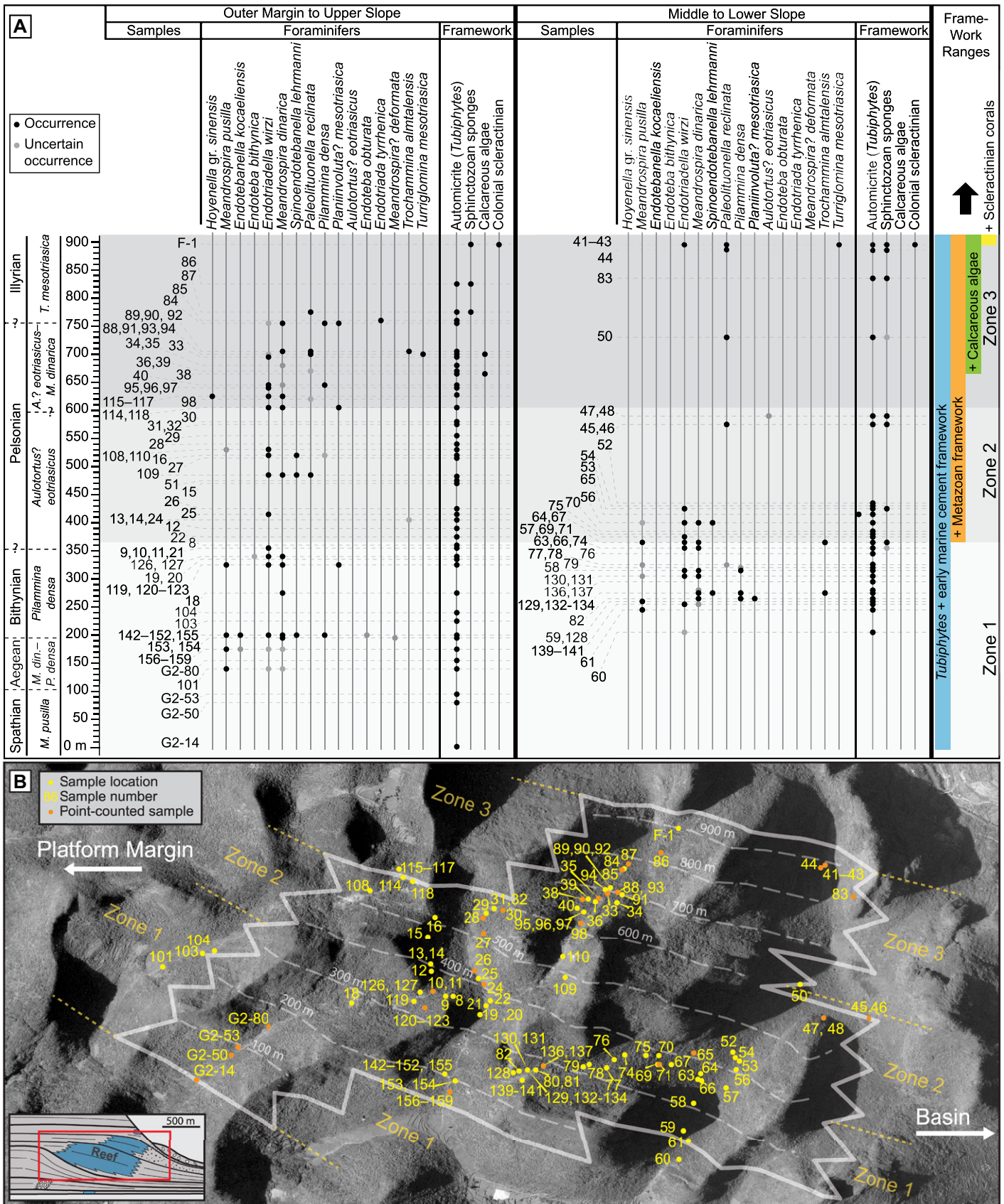


**Figure 3. (A) Biota occurrences. (B) Reef facies extent and sample locations on WorldView-1 satellite imagery. Reef foraminifer zones are based on Altiner et al. (2021). Abbreviations: Spa.—Spathian; Aeg.—Aegean; *M. pusilla*—*Meandrospira pusilla*; *M. din.*—*Meandrospira dinarica*; *P. densa*—*Pilammina densa*; *A.? eotriasicus*—*Aulotortus? eotriasicus*; *T. mesotriastica*—*Turriglomina mesotriastica*; *Hoyenella gr. sinensis*—*Hoyenella grege sinensis*.**

## RESULTS

The biotic composition of the GBG reef differed as a function of stratigraphic height (Figs. 3A and 4). Cement and *Tubiphytes* dominated the zone 1 reef facies (Figs. 4A–4D; Table S1 in the Supplemental Material<sup>1</sup>). Zone 2 contained denser occurrences of *Tubiphytes* and larger, more morphologically complex specimens (Figs. 4E and 4F). The lowest stratigraphic occurrence of identifiable reef-building metazoans (calcareous sponges) coincides with the base of zone 2, 365 m above the reef base (Figs. 3 and 4G–4I). Sponges made only a minor volumetric framework contribution (typically <1%) to zone 2 samples, and they exclusively occurred on the middle to lower slope until zone 3 (Figs. 3 and 4G–4I; Table S1). Zone 3 samples contained larger *Tubiphytes* and sponges (Figs. 4J and 4K), the first framework-contributing calcareous algae (Fig. 4L; 665 m above the reef base), and the first scleractinian corals (Figs. 4M and 4N; 895 m above the reef base). The stratigraphic position of the first-occurring scleractinian corals was consistent between field (F-1; Figs. 3 and 4M) and sample observations (sample 43; Figs. 3 and 4N). Cement volume decreased with stratigraphic height as biotic framework (Fig. 4O; Table S1) and metazoan-algal framework (Fig. 4P; Table S1) increased. Zone 1 and 2 samples contained 1–3 groups of framework builders (Fig. 4Q), typically represented by *Tubiphytes* and sponges. Taxonomic richness and evenness increased in zones 2 and 3 (Figs. 4Q and 4R; Table S1), with zone 3 samples containing 2–4 framework taxa (Fig. 4Q). Zone 1 and 2 framework-builder size was <17 mm. In zone 3, the maximum size of non-scleractinian framework builders was ~40 mm (Fig. 4S). The first-occurring scleractinian coral colonies (Figs. 3, 4M, and 4N) were larger than all other framework builders (up to ~60 cm; not shown in Fig. 4S).

Differences in recovery metrics among reef zones 1–3 were generally statistically significant (one-way analysis of variance [ANOVA]; see supplemental text and Table S2). Tukey post-hoc calculations indicated that only non-adjacent zones (1 and 3) differed significantly. Break points in recovery metrics were generally asynchronous, but the first occurrence of metazoan framework (~365 m) and the shift to the Upper Reef facies (~605 m) were influential (Figs. 4O–4S).

## DISCUSSION

The stepwise first occurrences of reef-building taxa, gradual increases in recovery metrics,

and statistically significant differences in those metrics across only nonadjacent reef stratigraphic zones (Figs. 3 and 4O–4S; Table S2) suggest gradual assembly of Triassic metazoan-algal reefs. The timing of coral-sponge-algal reef framework development suggests delayed recovery until the upper Pelsonian or lower Illyrian, 2–4 m.y. after Bithynian carbon-cycle stabilization (Payne et al., 2004). Spathian global cooling to less extreme or variable temperatures (Sun et al., 2012), lowered atmospheric  $p\text{CO}_2$  (Bernier, 2006), and the reduced extent and frequency of anoxic conditions (Lau et al., 2016) (Figs. 1, 3, and 4).

Although the GBG reef represents only one example of Triassic reef development, it is the only known upper Spathian to upper Anisian platform-margin reef, and the biotic composition of other Anisian reefs with overlapping stratigraphic intervals suggests that it might be representative. For example, preliminary evaluations of coeval Yangtze Platform reefs north of the GBG indicate similar biotic occurrences (Payne et al., 2006). Beyond south China, the next-oldest Anisian reefs are the upper Bithynian North Dobrogea reef (Romania) and the Nakhlak carbonate mounds (Iran). In Romania, a metazoan-algal reef framework is absent, but bryozoans and sponges occur in reef sediment (Popa et al., 2014). In Iran, cement and *Tubiphytes* dominate the reef framework, but sponges also occur (Berra et al., 2012), similar to the coeval GBG reef composition.

Previous interpretations of rapid middle Anisian metazoan-algal reef recovery in the Western Tethys region (e.g., Flügel and Senowbari-Daryan, 2001; Flügel, 2002) could reflect less favorable early Anisian depositional environments or the limitations of the Lower Triassic to lower Anisian carbonate stratigraphic record. A regional low-stand reduced accommodation and delayed carbonate platform development in the Western Tethys Ocean through the earliest Anisian (Emmerich et al., 2005). Thus, Anisian reefs there could reflect a later, more advanced stage of Triassic reef recovery that postdates much of the GBG reef.

In contrast to reefs, other benthic ecosystems and nektonic organisms such as conodonts, ammonoids, and fish show signs of more rapid Early Triassic diversification (e.g., Brayard et al., 2009; Dai et al., 2023). The absence of biodiverse metazoan-algal reefs during the same intervals implies that reef recovery required more favorable or stable environments, and the high preservation potential of reef-building organisms suggests that the observed reef pattern does not result from a biased fossil record. Alternatively, metazoan-algal reef recovery could have been delayed by the time required for the origination of new reef-building taxa or the advent of calcification in existing taxa, such as

the soft-bodied cnidarians that likely preceded scleractinian corals (Stanley, 2003).

Finally, although Middle Triassic reef recovery has been attributed to the development of high-relief platform topography and its impact on cementation (Velledits et al., 2011; Martindale et al., 2019), Early Triassic GBG platform-margin environments that lacked reefs were already characterized by high platform-to-basin relief (600 m; Kelley et al., 2020) and high carbonate saturation (e.g., Li et al., 2021), suggesting that Triassic reef recovery was decoupled from platform topography.

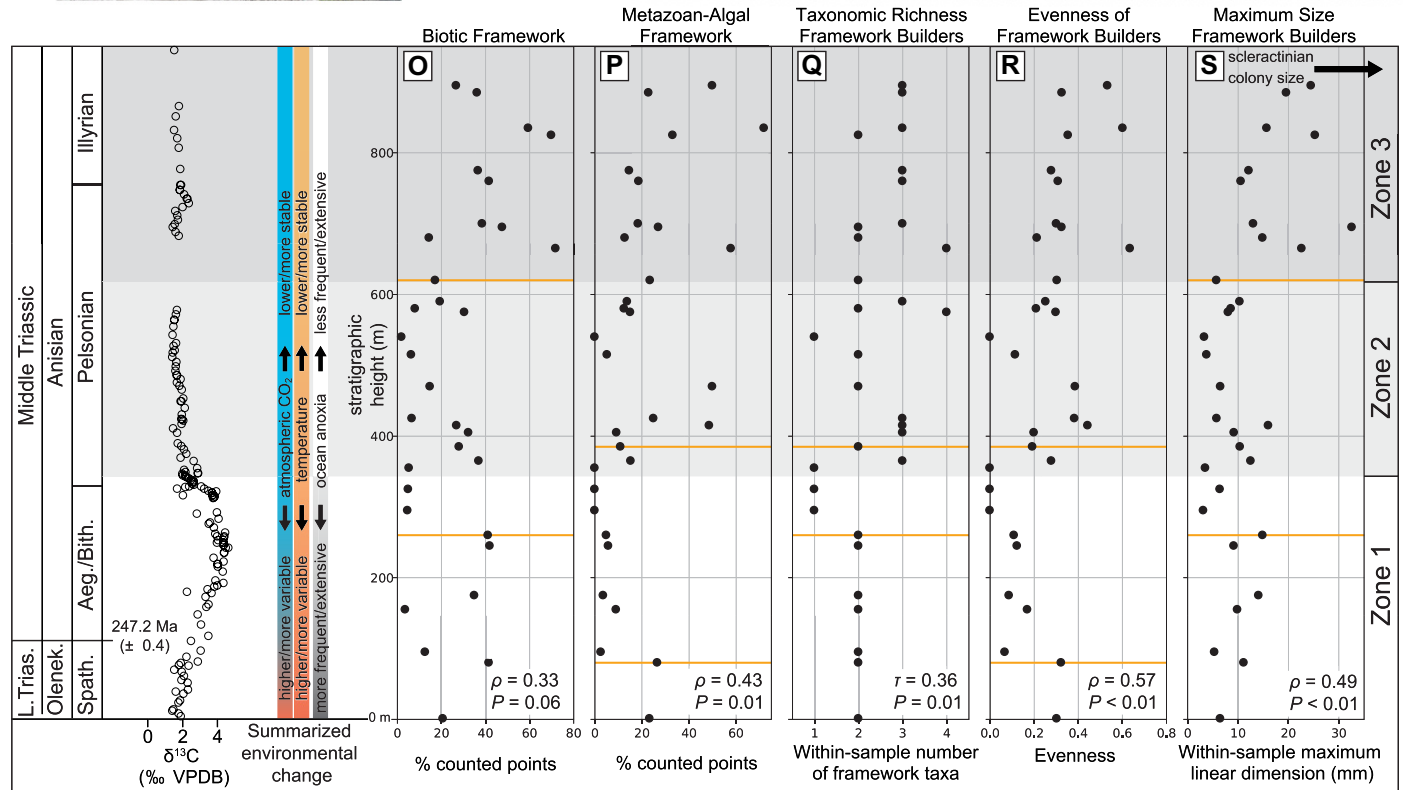
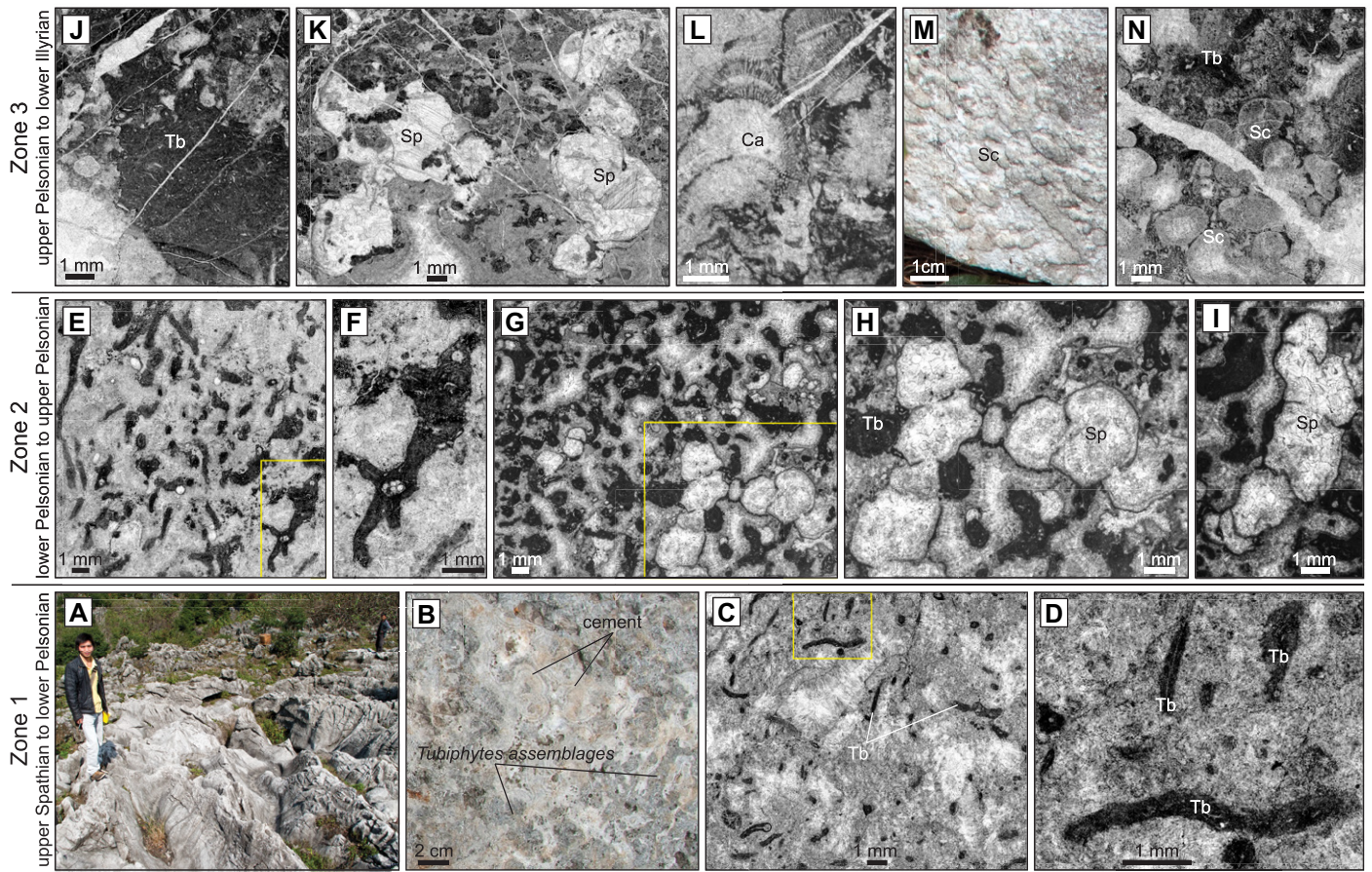
## SUMMARY AND CONCLUSIONS

Stepwise first occurrences in metazoan-algal reef builders and slow increases in biotic recovery metrics indicate a gradual rather than geologically rapid Triassic reef recovery. The delay in recovery compared to nonreef ecosystems suggests that reefs differ in their recovery tempo and might require more favorable or stable recovery environments. Our findings imply

**Figure 4. (A–N) Reef lithology and biota. Thin-section photomicrographs unless otherwise indicated. (A–D) Reef zone 1; (E–I) reef zone 2; (J–N) reef zone 3. Abbreviations: Tb—*Tubiphytes*; Sp—sponge; Ca—calcareous alga; Sc—scleractinian coral. (A) Reef exposure. (B) Outcrop example of reef framework. Dark-gray masses contain *Tubiphytes*. Light-gray to white masses are early marine cement. (C) Zone 1 *Tubiphytes* and cement boundstone. (D) Detail of yellow rectangle in C. (E) Zone 2 boundstone with denser occurrences of larger *Tubiphytes* specimens. (F) Detail of yellow rectangle in E showing increased size and morphological complexity of zone 2 *Tubiphytes* specimens. (G–I) Sample 71 *Tubiphytes* and calcareous sponge boundstone. (G) *Tubiphytes*-sponge boundstone framework. (H) Sponge detail of yellow rectangle in G. (I) Sponge detail. (J) Zone 3 boundstone showing larger and denser accumulations of *Tubiphytes*. (K) Larger and more volumetrically abundant zone 3 sponges. (L) Probable calcareous alga. Sample 93. (M) Outcrop colonial scleractinian coral specimen. (N) Scleractinian coral and *Tubiphytes* boundstone. (O–S) Reef-recovery metrics, with  $\delta^{13}\text{C}$  values from Payne et al. (2004). Age model is based on Lehrmann et al. (2015), Kelley et al. (2020), and Altner et al. (2021). Summarized and simplified changes in temperature, anoxia, and  $p\text{CO}_2$  are based on Sun et al. (2012), Lau et al. (2016), Lehrmann et al. (2022), and Bernier (2006). Orange lines in parts O to S represent Jenks natural break points. (O) Percentage of within-sample biotic reef framework points. (P) Percentage of metazoan, calcareous algae, or unidentifiable metazoans and calcareous algae in biotic reef framework points. Total biotic framework includes *Tubiphytes*. (Q) Taxonomic richness of *Tubiphytes*, sponge, calcareous alga, coral, and unidentified framework builders. (R) Framework evenness. (S) Maximum linear dimension of the largest within-sample framework builder. Olenek.—Olenekian; Spa.—Spathian; Aeg.—Aegean; Bith.—Bithynian; VPDB—Vienna Peedee belemnite.**

<sup>1</sup>Supplemental Material. Statistical analyses and tables. Please visit <https://doi.org/10.1130/GEOL.S.23751168> to access the supplemental material, and contact [editing@geosociety.org](mailto:editing@geosociety.org) with any questions.





that the degradation of modern reef ecosystems, if ultimately severe enough, could require a reef recovery interval lasting as long as several million years.

#### ACKNOWLEDGMENTS

This study was supported by the National Science Foundation (EAR-0807377-007 to J.L. Payne), the American Chemical Society (45329 to J.L. Payne; 40948-B2 and 33122-B8 to D.J. Lehrmann), the

National Geographic Society (8102-06 to J.L. Payne); and Shell (46000572 to D.J. Lehrmann). We thank Fu Hongbin, Deng Fan, and Liu Lingyun for field assistance. We thank William Foster and two anonymous reviewers for improving the original manuscript.

## REFERENCES CITED

- Altner, D., Payne, J.L., Lehrmann, D.J., Özkan-Altner, S., Kelley, B.M., Summers, M.M., and Yu, M., 2021, Triassic foraminifera from the Great Bank of Guizhou, Nanpanjiang Basin, south China: Taxonomic account, biostratigraphy, and implications for recovery from end-Permian mass extinction: *Journal of Paleontology*, v. 95, p. 1–53, <https://doi.org/10.1017/jpa.2021.10>.
- Baud, A., Richoz, S., Brandner, R., Krystyn, L., Heindel, K., Mohtat, T., Mohtat-Aghai, P., and Horaček, M., 2021, Sponge takeover from end-Permian mass extinction to early Induan time: Records in central Iran microbial buildups: *Frontiers of Earth Science*, v. 9, <https://doi.org/10.3389/feart.2021.586210>.
- Berner, R.A., 2006, GEOCARBSULF: A combined model for Phanerozoic atmospheric O<sub>2</sub> and CO<sub>2</sub>: *Geochimica et Cosmochimica Acta*, v. 70, p. 5653–5664, <https://doi.org/10.1016/j.gca.2005.11.032>.
- Berra, F., Balini, M., Levera, M., Nicora, A., and Salamati, R., 2012, Anatomy of carbonate mounds from the middle Anisian of Nakhlak (central Iran): Architecture and age of a subtidal microbial-bioclastic carbonate factory: *Facies*, v. 58, p. 685–705, <https://doi.org/10.1007/s10347-012-0299-z>.
- Brayard, A., Escarguel, G., Bucher, H., Monnet, C., Brühwiler, T., Goudemand, N., Galfetti, T., and Guex, J., 2009, Good genes and good luck: Ammonoid diversity and the end-Permian mass extinction: *Science*, v. 325, p. 1118–1121, <https://doi.org/10.1126/science.1174638>.
- Brayard, A., Vennin, E., Olivier, N., Bylund, K.G., Jenks, J., Stephen, D.A., Bucher, H., Hofmann, R., Goudemand, N., and Escarguel, G., 2011, Transient metazoan reefs in the aftermath of the end-Permian mass extinction: *Nature Geoscience*, v. 4, p. 693–697, <https://doi.org/10.1038/ngeo1264>.
- Dai, X., et al., 2023, A Mesozoic fossil lagerstätte from 250.8 million years ago shows a modern-type marine ecosystem: *Science*, v. 379, p. 567–572, <https://doi.org/10.1126/science.adf1622>.
- Emmerich, A., Zamparelli, V., Bechstäd, T., and Zühlike, R., 2005, The reefal margin and slope of a Middle Triassic carbonate platform: The Latemar (Dolomites, Italy): *Facies*, v. 50, p. 573–614, <https://doi.org/10.1007/s10347-004-0033-6>.
- Erwin, D.H., 1998, The end and the beginning: Recoveries from mass extinctions: *Trends in Ecology & Evolution*, v. 13, p. 344–349, [https://doi.org/10.1016/S0169-5347\(98\)01436-0](https://doi.org/10.1016/S0169-5347(98)01436-0).
- Flügel, E., 2002, Triassic reef patterns, in Flügel, E., et al., eds., *Phanerozoic Reef Patterns: Society for Sedimentary Geology (SEPM) Special Publication 72*, p. 391–463, <https://doi.org/10.2110/pec.02.72.0391>.
- Flügel, E., 2010, *Microfacies of Carbonate Rocks: Analysis, Interpretation and Application*: Berlin, Germany, Springer-Verlag, 984 p., <https://doi.org/10.1007/978-3-642-03796-2>.
- Flügel, E., and Senowbari-Daryan, B., 2001, Triassic reefs of the Tethys, in Stanley, G.D., ed., *The History and Sedimentology of Ancient Reef Systems (Topics in Geobiology Volume 17)*: Boston, Massachusetts, Springer, p. 217–249, [https://doi.org/10.1007/978-1-4615-1219-6\\_7](https://doi.org/10.1007/978-1-4615-1219-6_7).
- Heindel, K., et al., 2018, The formation of microbial-metazoan bioherms and biostromes following the latest Permian mass extinction: *Gondwana Research*, v. 61, p. 187–202, <https://doi.org/10.1016/j.gr.2018.05.007>.
- Heuer, F., Leda, L., Moradi-Salimi, H., Gliwa, J., Hairapetian, V., and Korn, D., 2022, The Permian-Triassic boundary section at Baghuk Mountain, central Iran: Carbonate microfacies and depositional environment: *Palaeobiodiversity and Palaeoenvironments*, v. 102, p. 331–350, <https://doi.org/10.1007/s12549-021-00511-1>.
- Kelley, B.M., et al., 2020, Controls on carbonate platform architecture and reef recovery across the Palaeozoic to Mesozoic transition: A high-resolution analysis of the Great Bank of Guizhou: *Sedimentology*, v. 67, p. 3119–3151, <https://doi.org/10.1111/sed.12741>.
- Lau, K.V., Maher, K., Altner, D., Kelley, B.M., Kump, L.R., Lehrmann, D.J., Silva-Tamayo, J.C., Weaver, K.L., Yu, M., and Payne, J.L., 2016, Marine anoxia and delayed Earth system recovery after the end-Permian extinction: *Proceedings of the National Academy of Sciences of the United States of America*, v. 113, p. 2360–2365, <https://doi.org/10.1073/pnas.1515080113>.
- Lehrmann, D.J., Wei, J., and Enos, P., 1998, Controls on facies architecture of a large Triassic carbonate platform: The Great Bank of Guizhou, Nanpanjiang Basin, south China: *Journal of Sedimentary Research*, v. 68, p. 311–326, <https://doi.org/10.2110/jsr.68.311>.
- Lehrmann, D.J., et al., 2015, An integrated biostratigraphy (conodonts and foraminifers) and chronostratigraphy (paleomagnetic reversals, magnetic susceptibility, elemental chemistry, carbon isotopes and geochronology) for the Permian–Upper Triassic strata of Guandao section, Nanpanjiang Basin, south China: *Journal of Asian Earth Sciences*, v. 108, p. 117–135, <https://doi.org/10.1016/j.jseas.2015.04.030>.
- Lehrmann, D.J., Stepchinski, L.M., Wolf, H.E., Li, L., Li, X., Minzoni, M., Yu, M., and Payne, J.L., 2022, The role of carbonate factories and sea water chemistry on basin-wide ramp to high-relief carbonate platform evolution: Triassic, Nanpanjiang Basin, south China: *The Depositional Record: A Journal of Biological, Physical and Geochemical Sedimentary Processes*, v. 8, p. 386–418, <https://doi.org/10.1002/dep2.166>.
- Li, X., Trower, E.J., Lehrmann, D.J., Minzoni, M., Kelley, B.M., Schaal, E.K., Altner, D., Yu, M., and Payne, J.L., 2021, Implications of giant ooids for the carbonate chemistry of Early Triassic seawater: *Geology*, v. 49, p. 156–161, <https://doi.org/10.1130/G47655.1>.
- Marengo, P.J., Griffin, J.M., Fraiser, M.L., and Clapham, M.E., 2012, Paleocology and geochemistry of Early Triassic (Spathian) microbial mounds and implications for anoxia following the end-Permian mass extinction: *Geology*, v. 40, p. 715–718, <https://doi.org/10.1130/G32936.1>.
- Martindale, R.C., Foster, W.J., and Velledits, F., 2019, The survival, recovery, and diversification of metazoan reef ecosystems following the end-Permian mass extinction event: *Palaeogeography, Palaeoclimatology, Palaeoecology*, v. 513, p. 100–115, <https://doi.org/10.1016/j.palaeo.2017.08.014>.
- Morycowa, E., and Szulc, J., 2010, Environmental controls on growth of early scleractinian patch reefs (Middle Triassic; Silesia; Poland): *Palaeoworld*, v. 19, p. 382–388, <https://doi.org/10.1016/j.palwor.2010.08.002>.
- Novack-Gottshall, P.M., 2008, Using simple body-size metrics to estimate fossil body volume: Empirical validation using diverse Paleozoic invertebrates: *Palaios*, v. 23, p. 163–173, <https://doi.org/10.2110/palo.2007.p07-017r>.
- Payne, J.L., Lehrmann, D.J., Wei, J., Orchard, M.J., Schrag, D.P., and Knoll, A.H., 2004, Large perturbations of the carbon cycle during recovery from the end-Permian extinction: *Science*, v. 305, p. 506–509, <https://doi.org/10.1126/science.1097023>.
- Payne, J.L., Lehrmann, D.J., Christensen, S., Wei, J., and Knoll, A.H., 2006, Environmental and biological controls on the initiation and growth of a Middle Triassic (Anisian) reef complex on the Great Bank of Guizhou, Guizhou Province, China: *Palaios*, v. 21, p. 325–343, <https://doi.org/10.2110/palo.2005.P05-58e>.
- Popa, L., Panaiotu, C.E., and Grădinaru, E., 2014, An early middle Anisian (Middle Triassic) *Tubiphytes* and cement crusts-dominated reef from North Dobrogea (Romania): Facies, depositional environment and diagenesis: *Acta Geologica Polonica*, v. 64, p. 189–206, <https://doi.org/10.2478/agp-2014-0011>.
- Pruss, S.B., Payne, J.L., and Bottjer, D.J., 2007, *Placunopsis* bioherms: The first metazoan buildups following the end-Permian mass extinction: *Palaios*, v. 22, p. 17–23, <https://doi.org/10.2110/palo.2005.p05-050r>.
- Scotese, C.R., 2014, Atlas of Middle & Late Permian and Triassic Paleogeographic Maps: Maps 43–48 from Volume 3 of the PALEOMAP Atlas for ArcGIS (Jurassic and Triassic) and Maps 49–52 from Volume 4 of the PALEOMAP PaleoAtlas for ArcGIS (Late Paleozoic), Mollweide Projection: Evanston, Illinois, PALEOMAP Project, 10 p., <https://doi.org/10.13140/2.1.2609.9209>.
- Senowbari-Daryan, B., 2013, *Tubiphytes* Maslov, 1956 and description of similar organisms from Triassic reefs of the Tethys: *Facies*, v. 59, p. 75–112, <https://doi.org/10.1007/s10347-012-0353-x>.
- Stanley, G.D., Jr., 1988, The history of early Mesozoic reef communities: A three-step process: *Palaios*, v. 3, p. 170–183, <https://doi.org/10.2307/3514528>.
- Stanley, G.D., Jr., 2003, The evolution of modern corals and their early history: *Earth-Science Reviews*, v. 60, p. 195–225, [https://doi.org/10.1016/S0012-8252\(02\)00104-6](https://doi.org/10.1016/S0012-8252(02)00104-6).
- Sun, Y., Joachimski, M.M., Wignall, P.B., Yan, C., Chen, Y., Jiang, H., Wang, L., and Lai, X., 2012, Lethally hot temperatures during the Early Triassic greenhouse: *Science*, v. 338, p. 366–370, <https://doi.org/10.1126/science.1224126>.
- Velledits, F., Péro, C., Blau, J., Senowbari-Daryan, B., Kovács, S., Piros, O., Pocsai, T., Szügyi-Simon, H., Dumitrică, P., and Pálffy, J., 2011, The oldest Triassic platform margin reef from the Alpine-Carpathian region (Aggtelek, NE Hungary): Platform evolution, reefal biota and biostratigraphic framework: *Rivista Italiana di Paleontologia e Stratigrafia*, v. 117, p. 221–268, <https://doi.org/10.13130/2039-4942/5973>.
- Wu, S., Chen, Z.-Q., Su, C., Fang, Y., and Yang, H., 2022, Keratose sponge fabrics from the lowermost Triassic microbialites in south China: Geobiologic features and Phanerozoic evolution: *Global and Planetary Change*, v. 211, <https://doi.org/10.1016/j.gloplacha.2022.103787>.

Printed in the USA